Waveguiding Effect in Electroabsorption Modulators: Passivation Layers and Their Impact on Extinction Ratios

Dong-Soo Shin

Waveguide structures of the stand-alone electroabsorption (EA) modulator and the electro-absorption modulated laser (EML) are investigated using the 3D beam propagation method. The EA waveguide structures with InP-based passivation layers show saturation in the extinction ratio (ER) due to the stray light traveling through the passivation layers. This paper demonstrates that narrower passivation layers suppress stray-light excitation in the EA waveguide, increasing the ER. A taper structure in the isolation section of the EML waveguide can reduce the mode mismatch and suppress the excitation of the stray light, increasing the ER further. Low-index-polymer passivation layers can confine the mode more tightly in the active waveguide, yielding an even higher ER.

Keywords: Electroabsorption (EA), waveguide, passivation, extinction ratio (ER).

Manuscript received May 06, 2004; revised July 26, 2004.

Dong-Soo Shin (phone: +82 31 400 5488, email: dshin@hanyang.ac.kr) is with the Department of Applied Physics, Hanyang University, Ansan, Gyeonggi, Korea.

I. Introduction

Electroabsorption modulators (EAMs) have been used in optical fiber communication systems due to their many advantages including small size, small driving voltage, polarization insensitivities, and possibility of integration with laser diodes [1]. There have been many investigations on the design of the active electroabsorption (EA) layer, particularly using quantum wells, to make the modulator more efficient [2], less polarization sensitive [3], or less susceptible to high optical power [4], for instance.

Since the EAM is a waveguide device, the waveguiding effect also has an important impact on the device performance. Previously, the stand-alone EAM was analyzed both experimentally and theoretically to show that the waveguiding effect can limit the device extinction ratio (ER) [5].

The ER of the EAM is an important parameter especially when the device is utilized to generate short pulses for return-to-zero data transmission [6] or for optical time division multiplexed systems [7]. A higher ER is preferred to prevent the inter-symbol or inter-channel interferences.

In this paper, the waveguiding effect in EA devices, not only in the stand-alone EAM, but also in the electroabsorption-modulated laser (EML), is examined using the 3D beam propagation method (BPM). Contrary to the prior work [5], a different approach, namely use of narrower passivation layers, is employed in this work to achieve a higher ER.

In [5], wider passivation layers were used to separate further the stray light traveling through the passivation layers from the active EA layers, thereby reducing the amount of stray light coupled to the output fiber. As a consequence, the ER was observed to increase after the light was coupled to the output fiber. In this work, it is shown that the narrower passivation

layers can suppress the stray-light excitation, thereby increasing the ER. The improvement suggested in this work is at the output facet of the EA waveguide, before the light is coupled to the output fiber. Other suggestions to improve the ER of the EAM and the EML are made, namely utilization of a taper in the EML waveguide structure and usage of a low-index polymer (LIP) as passivation layers.

In section II, the effect of ER saturation by the waveguiding is elucidated first. In section III, the 3D BPM simulations used in this work are explained. Then, in sections IV and V, the base EA waveguide and the EML waveguide structures are analyzed, respectively. Section VI summarizes and concludes the paper.

II. ER Saturation by Waveguiding

The ER is typically defined in dB as follows:

$$ER = 10\log\left(P_{on} / P_{off}\right), \tag{1}$$

where P_{on} and P_{off} are light powers (intensities) at on and off states, respectively. With the conventional formula for the attenuation due to the absorption coefficient α, which is a function of the applied voltage V on the EAM, the power $P(L,V)$ after the light travels distance L at a given voltage V is written as:

$$P(L,V) = P_0 \exp[-\Gamma\alpha(V)L]. \tag{2}$$

Here, P_0 is the initial light power, and Γ is the optical confinement factor at the EA layer.

If we take P_{on} and P_{off} as P_0 and $P(L,V)$, respectively, the ER at a given voltage (consequently at a given absorption coefficient) in dB is expressed as follows:

$$ER = (10\log e)\Gamma\alpha L \quad [\text{dB}]. \tag{3}$$

Note that the ER increases linearly with the absorption coefficient as long as Γ does not change.

If there exists a higher order mode in the EA waveguide, this higher order mode can be the dominating mode once the fundamental mode is fully absorbed. Since the light traveling as a higher order mode have different Γ, typically smaller than that of the fundamental mode, the existence of the higher order mode will change the slope of the ER vs. α curve.

Therefore, on top of the electroabsorption saturation in the EA layer, which limits the amount of the absorbed power, the waveguiding effect can also limit the absorbed power. The combined effect will eventually set the limit on the ER of the optical modulators.

III. BPM Simulations

To simulate how the light is coupled from the fiber and propagates through the waveguide, a 3D BPM, in particular BeamPROP by RSoft, is used. BeamPROP is based on the implicit finite-difference BPM. Throughout the calculations, the *full transparent boundary condition* is used to eliminate the light radiated from the waveguide at the boundary of the calculation. The *vector mode* is set as 'semi,' and *polarization* is transverse electric. The *compute steps* for x (horizontal direction), y (vertical direction), and z (propagation direction) are 0.02, 0.02, and 0.2 μm, respectively.

To check the ER at a given absorption coefficient, the imaginary part of the refractive index of the active layer is increased from zero to non-zero values. The imaginary part of the refractive index, κ, is related to α as follows:

$$\alpha = \frac{2\omega}{c}\kappa = \frac{4\pi}{\lambda}\kappa, \tag{4}$$

where ω is the angular frequency of light, c is the speed of light in a vacuum, and λ is the light wavelength.

As a reference, a κ of 0.01 corresponds to an α of approximately 800 cm^{-1} at a wavelength of 1.55 μm. The transmitted optical powers with zero and non-zero imaginary indices are obtained from the BPM simulations and used to calculate the ER at a given imaginary index (1). The width of the passivation layers is also varied in order to see its impact on the ER.

IV. Base EA Waveguide Structure

The base EA waveguide structure is shown in Fig. 1. Note that the scales of the horizontal and vertical dimensions are not the same. All the refractive indices are for materials based on InP or the quaternary InGaAsP lattice-matched to InP at a light wavelength of 1.55 μm. The width of the center ridge waveguide is given as 1.2 μm. The thickness of the active layer (index n = 3.456) is assumed to be 0.1 μm. An additional layer (n = 3.337) is assumed on top of the active layer, which is a non-absorbing separate confinement layer. The ridge waveguide width is typically dictated by the frequency-response requirement since the junction area determines the device capacitance.

After the ridge-waveguide etching, passivation layers are assumed to be grown and etched again. The waveguide height is assumed to be approximately 3 μm. Slightly different refractive indices are used for InP to account for the index

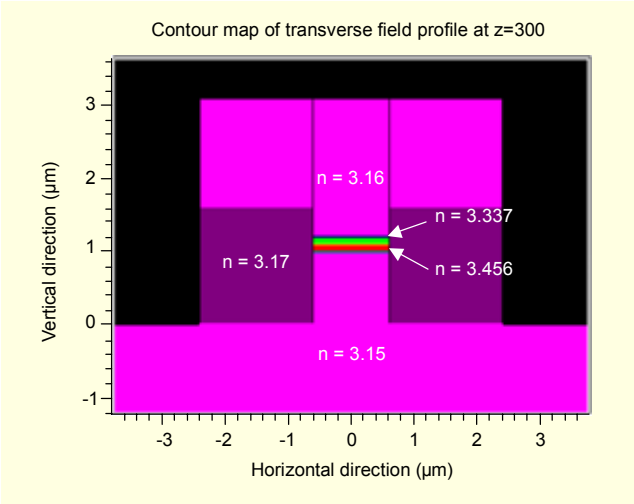

Fig. 1. Cross section of the base EA waveguide structure.

change due to doping. The layers with the refractive index n = 3.17 denote the Fe-doped InP. InP-based passivation layers are commonly used in industry to cover the waveguide sidewall, thereby protecting the active layer. When flip-chip bonding is employed for the packaging, the planarized passivation layers increase the contact area to the subassembly.

The width of the total waveguide (ridge + passivation) is 4.8 μm (passivation layers = 1.8 μm on each side). The center ridge waveguide structure given here is similar to the one considered in [5], but the passivation layers here are narrower than the ones given in [5] (3.8 μm on each side).

The detail of the calculated result may change with this particular waveguide structure, but the conclusion drawn from the calculation will be rather general. For example, one may want to use a thicker EA layer, which typically increases the optical confinement factor. Since what we are concerned with here is the lateral (horizontal) confinement of the mode by the passivation layers, not the vertical confinement, as changed by different EA-layer thickness, we would still have the similar impact on the ER with a thicker EA layer as well. This point will become clearer later in this section.

Three light powers are monitored in BPM simulations to see how the light propagates through the waveguide. First, the power in the active (center) ridge waveguide is monitored (Monitor 1). Second, the power in the passivation layers is monitored (Monitor 2). Monitor 3 is set to be the sum of Monitor 1 and Monitor 2, which is the power in the total waveguide.

A Gaussian beam with a free-space wavelength of 1.55 μm and a spot size of 1 μm is launched at the input facet of the waveguide. Figure 2 shows the Monitors as a function of the propagation length, z. A rather large mode mismatch exists between the fundamental mode of the waveguide and the input Gaussian beam that simulates the beam profile launched from the single-mode fiber with cylindrical symmetry. The launched Gaussian beam generates the higher mode as well as the fundamental mode. It can be seen in Fig. 2 that the portion of the power is transferred back and forth between the ridge waveguide and the passivation layers.

This beating occurs because the effective indices of the fundamental and higher order modes are different. The amount of this beating signifies the degree of higher-order-mode excitation. In [5], the degree of higher-order-mode excitation was experimentally verified by measuring the interference effect between the fundamental and higher order modes in the transmitted optical power. In this work, the higher-order-mode excitation manifests itself in the beating along the waveguide. From the beat length of approximately 45 μm, an effective index difference of approximately 0.034 is estimated. The simulated effective index of the fundamental mode is 3.441.

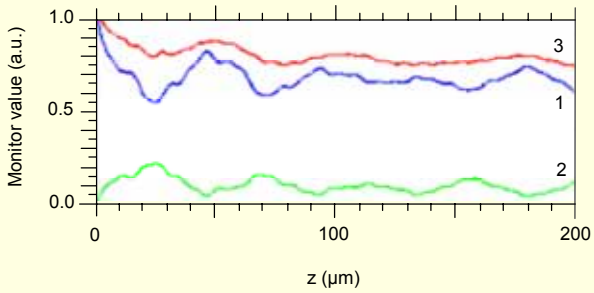

Fig. 2. Monitors as a function of the propagation length for the base EA waveguide structure. Each monitor is denoted by 1, 2, and 3.

Figures 3(a) and 3(b) show snapshots of the beam profile at two different positions in the waveguide. Figure 3(a) is a snapshot at a position where the power in the active waveguide is close to maximum. Figure 3(b) is at a position where the power in the active waveguide is close to minimum. It can be seen that the beam profile changes along the waveguide as the power is transferred between the active waveguide and the passivation layers as show in Fig. 2.

Figure 4 shows the simulated ER change with the imaginary refractive index. The width of the passivation layers are denoted as the trench width in the figure. The trench width is varied from 1.8 (as shown in Fig. 1) to 5 μm on each side, which increases the total waveguide width from 4.8 to 11.2 μm. As the imaginary refractive index increases from zero, the ER initially increases linearly as expressed in (3). The Γ of approximately 0.13 is obtained from the linear part of the curve in Fig. 4, which is for the fundamental mode.

A further increase in the imaginary index, however, does not

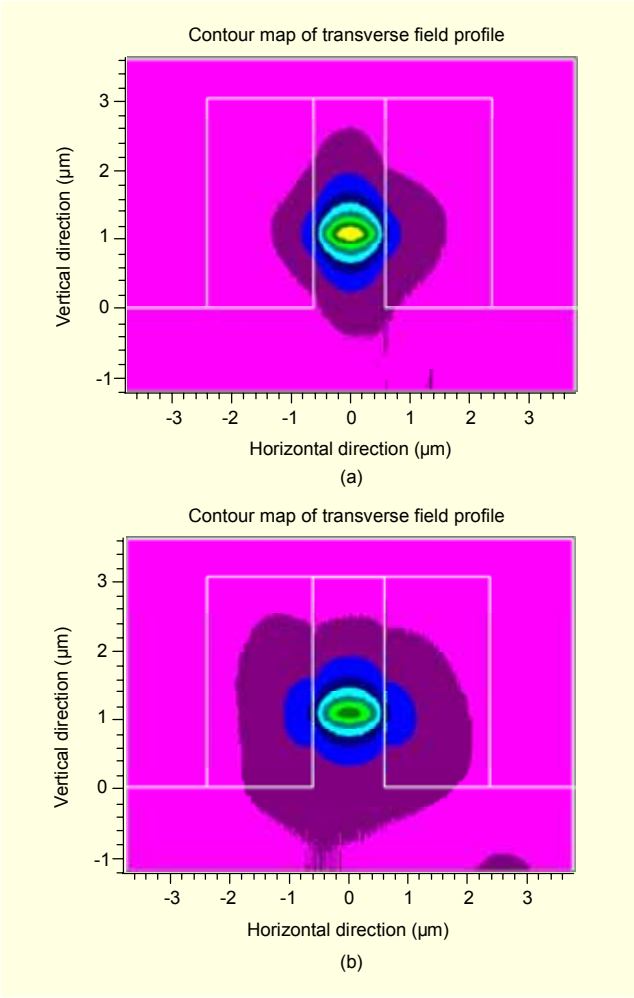

Fig. 3. Snapshots of the beam profile (a) when the power in the active waveguide is near maximum and (b) when the power in the active waveguide is near minimum for the base EA waveguide structure. The white lines represent the outlines of the waveguide.

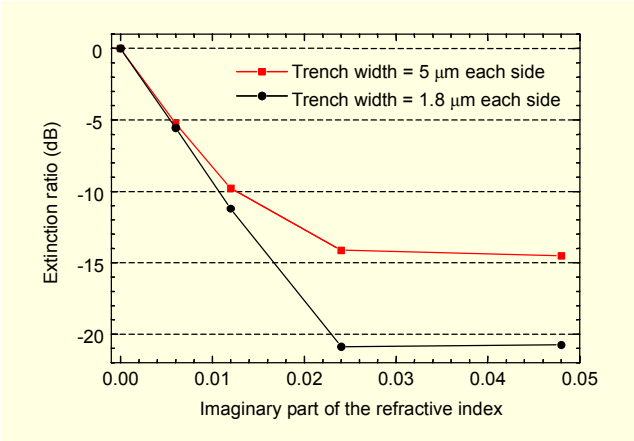

Fig. 4. ER as a function of the imaginary refractive index when the trench width (width of the passivation layer) is varied from 1.8 to 5 μm on each side for the base EA waveguide structure.

induce a linear increase in the ER; both trench widths show eventual saturation in the ER. The higher order mode is playing a dominant role in the saturation region after the light power in the fundamental mode is fully absorbed, as shown in section II. For this higher order mode, Γ is seen to be nearly zero. This means that the higher order mode does not have much overlap with the EA layer.

Figure 4 also shows that a narrower trench width has saturation in the ER at a higher ER value. From the saturated ER, the amount of power carried by the higher order mode is calculated to be 3.5 and 0.8% of the total waveguide power for the trench widths of 5 and 1.8 μm, respectively.

Figures 5(a) and 5(b) show the beam profiles for the trench widths of 1.8 and 5 μm on each side, respectively, when κ = 0.024. They show both the fundamental and higher order modes. We can see that the optical power carried by the higher

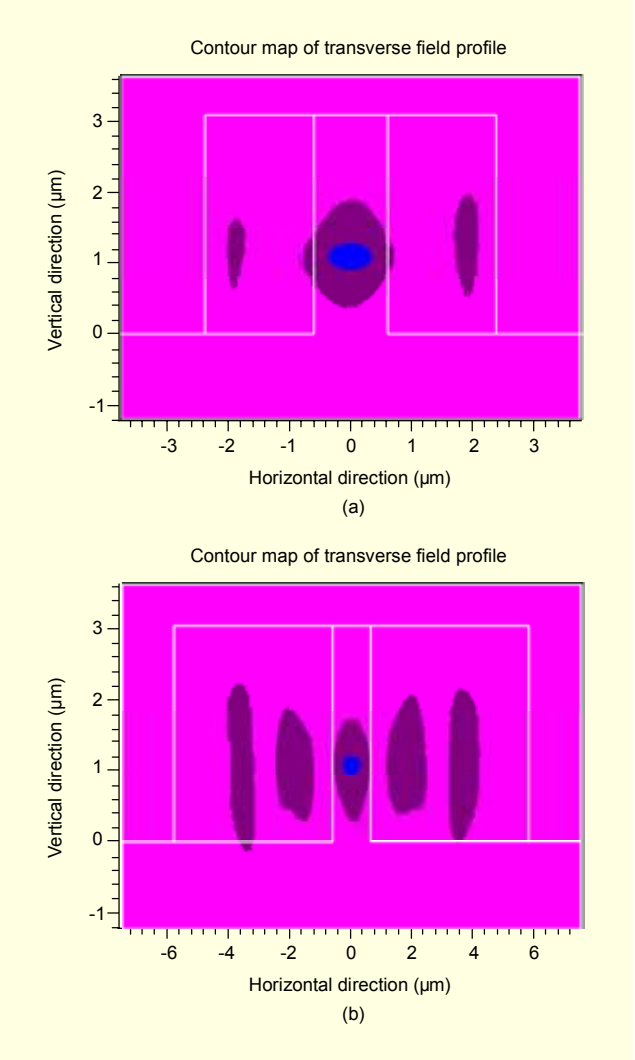

Fig. 5. Snapshots of the beam profile in the base EA waveguide with trench widths of (a) 1.8 μm and (b) 5 μm on each side when κ= 0.024.

order mode mainly propagates through the passivation layers. Thus, this higher order mode is sometimes called a (stray) lateral mode. We can also see from Fig. 5 that the narrower trench carries less power in the higher order mode than the wider trench. This fact is consistent with the result shown in Fig. 4. From the results shown in Figs. 4 and 5, it can be said that the narrower passivation layers suppress the excitation of the lateral higher order mode.

Even wider (12 μm on each side) passivation layers and a deeply etched ridge (5 μm) were used in [5] to separate the stray lateral mode from the active ridge waveguide further so that less power may be coupled to the output fiber for the lateral mode. Although this approach does not suppress the excitation of the lateral mode from the EA waveguide, it was reported that the ER measured from the optical power coupled to the output fiber indeed increased. Another approach utilized the InGaAs absorption layer situated 1.4 μm beneath the EA layer to selectively absorb the higher-order parasitic mode [8].

The present work is contrasted with [5] as it tries to suppress the higher-order lateral mode using narrower passivation layers to increase the ER of the EAM. By using narrower passivation layers, the lateral higher order mode can be attenuated further due to the sidewall roughness, which is not taken into account in the simulations here.

V. EA Waveguide Structure in the EML

In the EML, the input light to the EA waveguide structure is from the diode laser monolithically integrated with the EAM. Since the laser waveguide structure is quite close to that of the EAM, the mode mismatch between these two waveguides is greatly reduced.

The fundamental mode of the laser waveguide is first calculated with the BPM simulation. The laser waveguide structure considered herein has the same layers and width as the EA waveguide structure shown in Fig. 1, but the active layer is thicker (by approximately 50%) than that of the EA waveguide. InP-based passivation layers are also used on both sides of the ridge laser waveguide structure. The width of the passivation layers is fixed as 5 μm on each side. Since the active layer of the laser waveguide is a little thicker, the fundamental mode is tightly confined around the active layer. Figure 6 shows the profile of the laser fundamental mode.

Typically, an isolation section exists between the diode laser and the EAM to electrically isolate the two devices. In this simulation, an isolation section of approximately 200 μm is inserted in front of the EAM. The laser fundamental mode is then launched into the EA waveguide through the isolation section. The length of the EA waveguide is 150 μm.

Figure 7 shows Monitors as a function of the propagation

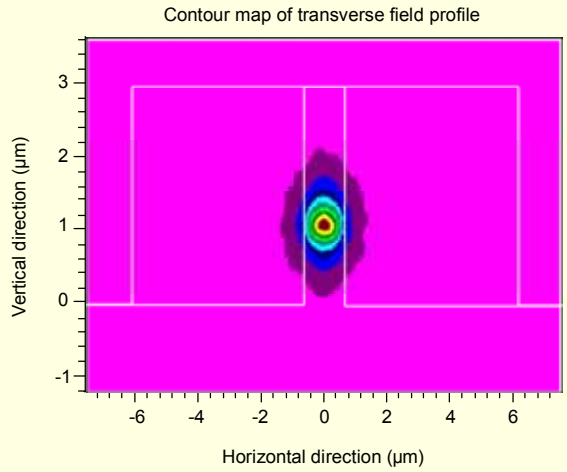

Fig. 6. Beam profile of the laser fundamental mode.

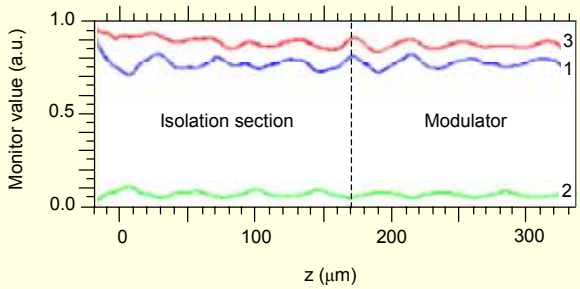

Fig. 7. Monitors along the propagation length for the EA waveguide structure in the EML. No taper is used.

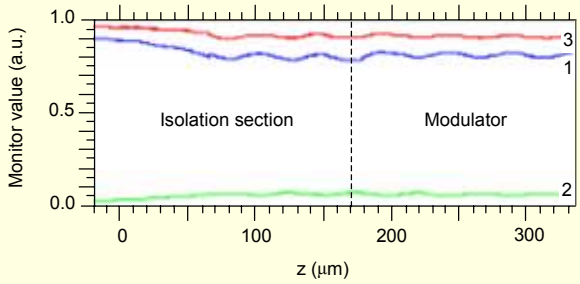

Fig. 8. Monitors along the propagation length for the EA waveguide structure in the EML. A linear taper is used.

length, z. It can be seen that the beating is significantly reduced, implying less power is coupled into the EA waveguide as the higher order mode than in the case shown in Fig. 2.

We can reduce the beating further by introducing a linear taper in the isolation section to transform the mode from the laser to the modulator more adiabatically. Figure 8 shows the case when we introduce the linear taper. The beating is even smaller than the case shown in Fig. 7. Shown in Fig. 9 is a snapshot of the beam profile in the EA waveguide, which is

quite close to the shape of the laser fundamental mode shown in Fig. 6, but expanded in size.

Figure 10 shows the ER calculation results for the waveguide with the linear taper. The ER is increased further for both trench widths, when compared with the result shown in Fig. 4. The saturated regions in Fig. 4 appear at a higher imaginary refractive index in Fig. 10, indicating that even less power is carried by the lateral higher order mode.

Different trench widths (widths of passivation layers) show a trend similar to the result in Fig. 4: narrower passivation layers show a higher ER. From the saturated ER, the amount of power carried by the higher order mode is calculated to be 0.9 and 0.2% of the total power for the trench widths of 5 and 1.8 μm, respectively.

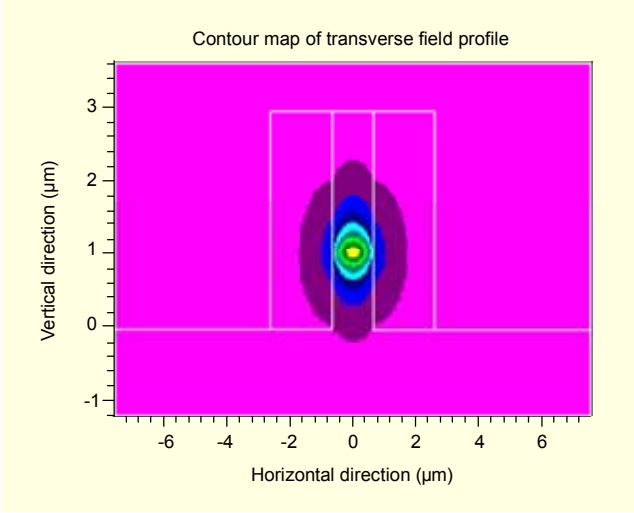

Fig. 9. Snapshot of the beam profile in the EA waveguide structure of the EML when the linear taper is used.

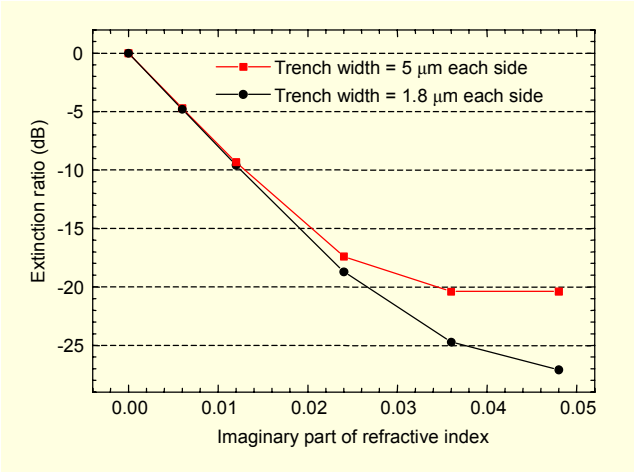

Fig. 10. ER as a function of the imaginary refractive index when the trench width is varied from 1.8 to 5 μm on each side for the EA waveguide structure in the EML. A linear taper is used.

To further suppress the excitation of the higher order mode, an LIP, e.g., polyimide or benzocyclobutene, can be used to confine the mode more tightly inside the active ridge waveguide. Figure 11 shows a calculation that compares the InP and LIP passivations (index of LIP = 1.5). For the same active ridge waveguide width of 1.2 μm, we can see that the ER improves by approximately 2 dB at the imaginary index of 0.024 by using the LIP instead of InP passivations (compare the circle with the inverted triangle).

When we relax the width of the active ridge waveguide to 2 μm, the ER increases by approximately 2 dB additionally at the same imaginary index (inverted triangle to triangle). This is because the wider ridge waveguide confines the beam within the active EA layer further, increasing the optical confinement factor, Γ. The increased Γ within the active EA layer is vindicated by the higher slope in the ER vs. imaginary refractive index shown in Fig. 11.

The LIP can also be used to increase the ER in a stand-alone EAM that has a rather large mode mismatch to the fiber in order to reduce the light power carried by the passivation layers.

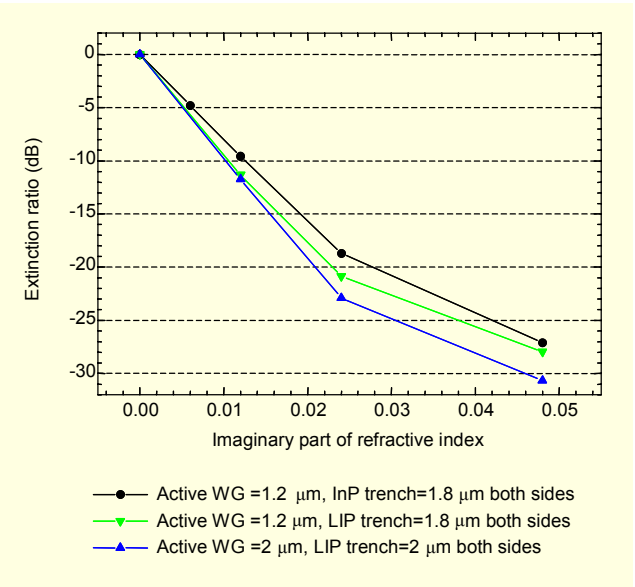

Fig. 11. ER as a function of the imaginary refractive index when the LIP is used as passivation layers in the EA waveguide of the EML. A linear taper is used.

VI. Conclusion

EA waveguide structures have been analyzed using 3D BPM simulations. The higher-order-mode excitation in the EA waveguide with InP passivation layers can cause an ER saturation in the EAM. Narrower passivation layers can be used to suppress the higher-order-mode excitation and increase the ER.

In the EML waveguide structures, an isolation section with a linear taper can be used to minimize the mode mismatch. Narrower passivation layers in the EA waveguide as well as the taper in the isolation section can be used in the EML to increase the ER. The ER can be increased further by using the LIP, instead of the InP, to passivate the sidewall as the waveguide with the LIP passivation can confine the light within the active waveguide more tightly.

References

[1] M. Aoki, M. Suzuki, H. Sano, T. Kawano, T. Ido, T. Taniwatari, K. Uomi, and A. Takai, "InGaAs/InGaAsP MQW Electroabsorption Modulator Integrated with a DFB Laser Fabricated by Band-Gap Energy Control Selective Area MOCVD," *IEEE J. Quantum Electron.*, vol. 29, no. 6, 1993, pp. 2088–2096.

[2] K.K. Loi, I. Sakamoto, X.B. Mei, C.W. Tu, and W.S.C. Chang, "High-Efficiency 1.3 μm InAsP-GaInP MQW Electroabsorption Waveguide Modulators for Microwave Fiber-Optics Links," *IEEE Photon. Technol. Lett.*, vol. 8, no. 5, 1996, pp. 626–628.

[3] A. Ougazzaden and F. Devaux, "Strained InGaAsP/InGaAsP/InAsP Multi-Quantum Well Structure for Polarization Insensitive Electroabsorption Modulator with High Power Saturation," *Appl. Phys. Lett.*, vol. 69, no. 27, 1996, pp. 4131–4132.

[4] D.S. Shin, W.X. Chen, Y. Zhuang, Y. Wu, S.A. Pappert, D. Chow, D. Yap, P. Deelman, and P.K.L. Yu, "Suppressing Electroabsorption with Intra-Step-Barrier Quantum Wells for High-Power Electroabsorption Modulators," *Electron. Lett.*, vol. 38, no. 19, 2002, pp. 1140–1142.

[5] D. G. Moodie, M. J. Harlow, M. J. Guy, S. D. Perrin, C. W. Ford, and M. J. Robertson, "Discrete Electroabsorption Modulators with Enhanced Modulation Depth," *J. Lightwave Technol.*, vol. 14, no. 9, 1996, pp. 2035–2043.

[6] A. Ougazzaden, C. W. Lentz, T. G. B. Mason, K. G. Glogovsky, C. L. Reynolds, G. J. Przybylek, R. E. Leibenguth, T. L. Kercher, J. W. Boardman, M. T. Rader, J. M. Geary, F. S. Walters, L. J. Peticolas, J. M. Freund, S. N. G. Chu, A. Sirenko, R. J. Jurchenko, M. S. Hybertsen, and L. J. P. Ketelsen, "40 Gb/s Tandem Electro-absorption Modulator," *Proc. Optical Fiber Communication Conference 2001* (*OFC 2001*), 2001, vol. 4, pp. PD14-1 – PD14-3.

[7] A. D. Ellis, M. C. Tatham, D. A. O. Davies, D. Nesset, D. G. Moodie, and G. Sherlock, "40 Gb/s Transmission over 202 km of Standard Fiber Using Mid Span Spectral Inversion," *Electron. Lett.*, vol. 31, no. 4, 1995, pp. 299 – 301.

[8] C. Rolland, G. Mak, W. Bardyszewski, and D. Yevick, "Improved Extinction Ratio of Waveguide Electroabsorption Optical Modulators Induced by an InGaAs Absorbing Layer," *J. Lightwave Technol.*, vol. 10, no. 12, 1992, pp. 1907–1911.

Dong-Soo Shin received the BS degree in physics from Yonsei University, Seoul, Korea in 1993, and the MS and PhD degrees in physics from the University of California, San Diego, California, USA in 1996 and 2001. From 2001 to 2003, he participated in the development of high-speed electroabsorption-modulated lasers (EMLs) and uncooled lasers as a Member of Technical Staff at Agere Systems (formerly Lucent Technologies Microelectronics), Breinigsville, Pennsylvania, USA. From 2003 to 2004, he worked as a Senior Scientist at SpatiaLight, Novato, California, USA, where he was involved with the research and development of microdisplays based on liquid crystal on Silicon (LCoS). In 2004, he joined the faculty of Applied Physics at Hanyang University, Ansan, Korea. His current research interests include optoelectronic devices and their novel applications, device physics, and microdisplays. Dr. Shin is a Member of the Institute of Electrical and Electronics Engineers (IEEE).